ELSEVIER

Journal of Power Sources 64 (1997) 175–180

JOURNAL OF POWER SOURCES

# Electrochemical modelling of lead/acid batteries under operating conditions of electric vehicles

Eckhard Karden *, Peter Mauracher, Friedhelm Schöpe

*Department of Power Electronics and Electrical Drives, Aachen University of Technology, Jägerstrasse 17–19, 52056 Aachen, Germany*

**Abstract**

In order to overcome deficiencies of phenomenological models of batteries for electric vehicles, this paper analyses models based on electrochemical laws. Considering one space coordinate, there are essentially two approaches: (i) macrohomogeneous and (ii) single-pore models. It is shown that they are equivalent under general assumptions. A macrohomogeneous model of a valve-regulated lead/acid battery is calculated for a highly dynamic discharge current pattern. Simulated voltage as a function of time matches experimental results, but further work is necessary, especially in a careful determination of several empirical parameters. Finally, battery models restricted to ordinary differential equations are discussed as an approximation of spatial models.

*Keywords:* Lead/acid batteries; Electrodes; Macrohomogeneous model; Single-pore model; Electric vehicles

## 1. Introduction

Battery models for engineering applications are usually phenomenological ones (e.g. electric equivalent circuits) whose main disadvantages are: (i) model parameters depend — in a complicated way — on battery-type fabrication, age, history, state-of-charge, current, temperature, etc., and (ii) a description of the battery behaviour by phenomenological 'black-box' models hardly improves the understanding of the underlying principles. Therefore, it is examined whether battery modelling for electric-vehicle (EV) applications can be improved by electrochemically based approaches.

Up to now, most simulations based on electrochemical models are restricted to constant-current conditions, and often to small deviations from thermodynamical equilibria (e.g. linearized Butler–Volmer equation). The current in EVs is high ($\approx 1 \ldots 10\, I_5$) and strongly dynamic in a time range of seconds; it does even change its direction for seconds due to regenerative braking.

## 2. One-dimensional modelling of porous electrodes

Battery electrodes are porous in order to maximize their surface-to-volume ratio and thus the reactive interface between electrode material and electrolyte. Models of transport and reaction in porous electrodes are mostly restricted to one spatial dimension for reasons of simplicity and to avoid time-consuming computing. In general, this space coordinate is chosen perpendicular to the outer electrode surface. We consider only plate electrodes which may be described in Cartesian coordinates. The plate is assumed as infinitely extended in the $(y, z)$ plane, and spatial inhomogeneities will be considered only along the third Cartesian axis, here called $x$ (Fig. 1).

There are two different kinds of one-dimensional models of porous electrodes [1,2]:

(i) A macrohomogeneous model describes the porous electrode as a superposition of two continua, the electrode matrix and the pore-filling electrolyte.

(ii) In a single-pore model the real porous structure is represented by identical tubes which are cylindrical, not interconnected, either straight or curved along their axis (Fig. 1).

Both models are based on averageing of the geometric details of the porous structure and might be summarized under the term 'mesoscopic'. In fact, both approaches are equivalent in one spatial dimension. This means that it is possible to transform any macrohomogeneous model into a single-pore model (and vice versa) which shows the same transport and reaction properties on a mesoscopic scale. Thus, macrohomogeneous and single-pore approaches use different terms to describe the same phenomenon [2]. However, dif-

* Corresponding author. Tel: +49-241-806945; Fax: +49-241-67505; e-mail: ka@isea.rwth-aachen.de.


*PII* S0378-7753(96)02518-9

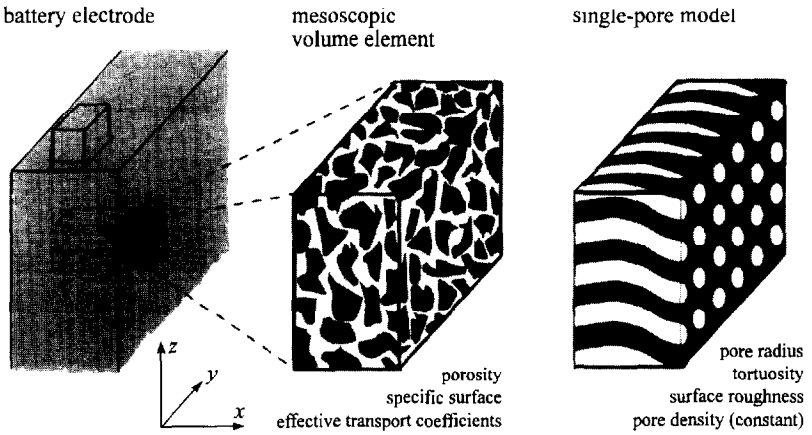


Fig. 1. One-dimensional modelling of porous electrodes: single-pore and macrohomogeneous approaches.

ferences between macrohomogeneous and single-pore approaches become significant by extending the model to two or three space dimensions [3,4].

For the special case of a one-dimensional porous structure which does not change in time, this equivalence was shown by Winsel [5]. In the following it is shown that both 'mesoscopic' approaches are equivalent even in the more general case of a battery electrode which undergoes a structural change during discharge/charge reactions. It is emphasized that one can change one model into the other using purely geometric considerations, regardless the physical or chemical properties of the electrode system.

In a first step, a porous-electrode model is set up based on the macrohomogeneous approach. Five basic assumptions are formulated which summarize different models, based on the macrohomogeneous and single-pore approaches. In a second step, all quantities characterizing this generalized macrohomogeneous model will be transformed to quantities describing a single-pore model.

The basic assumptions made for 'mesoscopic' modelling of porous electrodes are: (i) structure; (ii) structural changes; (iii) transport in the pores; (iv) transport in the matrix, and (v) and inter-phase currents.

### 2.1. Structure

*The electrode consists of two phases: liquid electrolyte and solid matrix (active material). The volume fraction of the electrolyte phase is called porosity.*

Solid substructures are not considered; they may modify the effective matrix conductivity. Although the gas phases are not considered, $O_{2(g)}$ transport in valve-regulated lead/acid (VRLA) batteries is sometimes taken into account by increasing the effective diffusion constant [6].

### 2.2. Structural change

*During electrochemical reaction(s) the structure of the electrode is changed fully reversibly. The state of each volume element is uniquely characterized by one scalar quantity, e.g. the porosity* $\epsilon$.

Reversibility means that the scalar quantity characterizing the structure of a volume element is a unique function of the time integral of electrochemical current within this volume element. The latter may be normalized and is then called local state-of-charge (SOC). The function $\epsilon$(SOC) is usually supposed to be linear; its parameters may depend on local current density.

### 2.3. Transport in the pores

*Electric conduction and ion diffusion (of one or more components) are described by transport equations analogous to those for the bulk electrolyte, but with modified ('effective') transport coefficients, such as conductivity* $\kappa$ *and diffusion constant D. This modification is, for each kind of transport, a multiplication with one and the same structure-dependent factor* $f_L(\epsilon)$: $\kappa_{eff}=f_L(\epsilon)\,\kappa_{bulk}$; $D_{eff}=f_L(\epsilon)\cdot D_{bulk}$, etc. where $f_L(\epsilon)$ accounts for a reduced cross section and longer transport paths (tortuosity) within the pores, compared with the bulk medium. In practice, only two forms are used for the structure-dependent factor:

(i) $f_L(\epsilon)=\epsilon/\theta^2$ where the labyrinth factor $\theta>1$. The path between two points in a tortuos single-pore is $\theta$ times longer than the straight connection between these points. This approach comes from modelling of time-invariant pore structures (see Ref. [5]) and may be generalized to pores of $x$-dependent cross section (constricted pore model [7]).

(ii) $f_L(\epsilon)=\epsilon^{ex}$ where $ex>1$, the tortuosity exponent. This approach is the typical one in recent macrohomogeneous models, see Refs. [8–10].

For battery electrodes, approach (ii) was in a better agreement with the experimental results [2,11]. This fact may be interpreted geometrically: during the discharge/charge reaction not only the cross section of the pores, but also the labyrinth factor $\theta$ is variable.

### 2.4. Transport in the matrix

*The effective electric conductivity* $\sigma$ *of the solid matrix equals also a structure-dependent factor times the conductiv-*

*ity of the bulk material. Diffusion in the solid phases is neglected or considered as part of the electrode kinetics*: $\sigma_{\text{eff}}=f_{\text{M}}(\epsilon)\sigma_{\text{bulk}}$.

The function $f_{\text{M}}(\epsilon)$ is less clear than the function $f_{\text{L}}(\epsilon)$, mainly caused by the fact that a battery electrode, in general, consists of at least two solid materials (charged and discharged species) which rarely form one phase. In the case of the $PbO_2/PbSO_4$ electrode (consisting of a semiconducting and an insulating phase), different macrohomogeneous models vary from $\sigma_{\text{eff}}$ increasing with local SOC [12] to $\sigma_{\text{eff}}$ decreasing with local SOC [8]. Single-pore models usually neglect the matrix resistance and assume constant potential within the matrix [1,3,5]. However, the model output does not strongly depend on these assumptions about transport in the solid matrix because the resistance of all solid parts of a lead/acid battery is small compared with the electrolyte resistance and non-ohmic losses.

### 2.5. Inter-phase currents

*An electric current can pass the electrolyte/matrix interface either through electrochemical reaction(s) or through double-layer capacity. It is assumed that the divergence of electric current density in the electrolyte phase, $\partial i_{\text{L}}/\partial x$, is determined by equations valid for flat electrodes, multiplied with the specific inner surface per unit volume $a(\epsilon)$ of the porous electrode. This factor contains the whole structural dependence*: $\partial i_{\text{L}}/\partial x=a(\epsilon)\{j_{\text{R}}+j_{\text{C}}\}$.

Electrode kinetics $j_{\text{R}}$ are described by Butler–Volmer-type equations, sometimes modified in order to account for a more complex reaction mechanism [9,10,13]. The capacitive current $j_{\text{C}}$ is very often neglected due to the short time constant formed by transfer resistance and double-layer capacity. This approximation is well justified for constant-current conditions [14] but should be carefully checked for pulsed discharge (cf. Ref. [9]) or other dynamic current patterns. The assumption given above implies also that the microscopic pore walls behave the same way as surfaces of flat electrodes. The function $a(\epsilon)$ is mostly assumed to be non-linear and may be explained by microscopic geometric models [15]. It may additionally depend on current density (local Peukert equation, see Ref. [16]).

Having set up the 'mesoscopic' model in terms of the macrohomogeneous approach, i.e. using average quantities such as effective conductivities and specific inner surface, we will now calculate the geometric parameters of a single-pore structure with the same transport and reaction properties. We will, however, neglect the matrix resistance according to the above discussion. The pore structure consists of $N$ identical pores per unit area of the $(y, z)$ plane which extend over the full plate 'thickness' $d$ along the $x$-direction. Each of the pores is characterized by its length $\theta d$, its radius $r$ (called equivalent radius), and its surface roughness $f_{\text{rough}}$. The number $N$ of pores will remain unchanged during the discharge/charge reaction. Thus, we have to determine three pore parameters $\theta$, $r$, $f_{\text{rough}}$ from three averaged quantities characterizing the variable electrode structure, $\epsilon$, $f_{\text{L}}(\epsilon)$, and $a(\epsilon)$.

We consider a mesoscopic volume element $\Delta x\Delta y\Delta z$ which is small compared with electrode dimensions, but big compared with pore dimensions. The volume fraction of $N\Delta y\Delta z$ pore segments, each of length $\theta\Delta x$ and cross section $\pi r^2$, within $\Delta x\Delta y\Delta z$ is

$$\epsilon=\frac{N\Delta y\Delta z\cdot\pi r^2\theta\Delta x}{\Delta x\Delta y\Delta z}=N\pi r^2\theta \tag{1}$$

Their specific surface equals the circumference times length per volume unit

$$a(\epsilon)=f_{\text{rough}}\frac{N\Delta y\Delta z\cdot 2\pi r\theta\Delta x}{\Delta x\Delta y\Delta z}=N2\pi r\theta \tag{2}$$

The transport coefficients, e.g. the diaphragm conductivity, of the single-pore structure is reduced, compared with $\Delta x\Delta y\Delta z$ filled with bulk electrolyte, by a factor of

$$f_L(\epsilon)=\frac{N\Delta y\Delta z\cdot\pi r^2}{\Delta y\Delta z}\Big/\frac{\theta\Delta x}{\Delta x}=\frac{N\pi r^2}{\theta} \tag{3}$$

Eqs. (1)–(3) are solved

$$r=\frac{1}{\sqrt{\pi N\theta}} \tag{4}$$

$$\theta=\sqrt{\frac{\epsilon}{f_{\text{L}}(\epsilon)}} \tag{5}$$

$$f_{\text{rough}}=\frac{a(\epsilon)}{2\epsilon\sqrt{\pi N\theta}} \tag{6}$$

Eqs. (4)–(6) define a class of single-pore structures with the properties demanded, because the pore density $N$ of the single-pore structure is not yet determined. It may be chosen appropriately in order to achieve an equivalent radius $r$ comparable with realistic pore dimensions.

## 3. Simulation of a VRLA battery

A one-dimensional mesoscopic model of a VRLA battery with gelled electrolyte (Sonnenschein dryfit 160 Ah) is set up similar to macrohomogeneous models reported in Refs. [6,16]. A set of five partial differential equations (PDE) represents (i) charge transport in the electrolyte, and (ii) in the electrode matrix, (iii) kinetics of the electrochemical charge/discharge reaction, (iv) transport of electrolyte, and (v) structural change of the porous electrodes. The dependent variables of this PDE system are: electric current density, $i$, in the electrolyte phase ($x$-direction), electric potentials, $\phi_{\text{L}}$ and $\phi_{\text{M}}$, in the electrolyte and the electrode phases, respectively, concentration, $c$, of the electrolyte, porosity, $\epsilon$, of the electrodes. In this paper, the oxygen cycle is not yet included. The battery is divided into four areas: two porous electrodes (POS, NEG), a gelled electrolyte reservoir (RES), and a

porous separator (SEP). The model equations used in our simulation are listed below. Comments can be found in Refs. [6,16].

### 3.1. Charge transport in the electrolyte phase

$$i_L = -\epsilon^{ex}\kappa\left[\frac{\partial\phi_L}{\partial x} - (1-2t_+^0)\frac{RT}{F}\frac{\partial \ln(f_\pm c)}{\partial x}\right]$$

in POS, RES, SEP, NEG (7)

$$\epsilon^{ex}\frac{\partial\phi_L}{\partial x} \text{ continuous at inner borders} \quad (8)$$

$$\frac{\partial\phi_L}{\partial x} = 0 \text{ at current collectors} \quad (9)$$

Eq. (7) is true for a concentrated, fully dissociated, binary electrolyte, with: $t_+^0$ the transference number of protons; $f_\pm$ the mean activity coefficient; $ex$ the tortuosity exponent; $R$ the universal gas constant; $T$ the absolute temperature, and $F$ the Faraday constant.

### 3.2. Charge transport in the matrix phase

$$I - i_L = -\epsilon^{exm}\sigma\frac{\partial\phi_M}{\partial x} \text{ in POS, NEG} \quad (10)$$

$$\phi_M = 0 \text{ in RES, SEP} \quad (11)$$

$$\left.\frac{\partial\phi_M}{\partial x}\right|_{\text{electrode}} = 0 \text{ inner borders (POS/RES, SEP/NEG)} \quad (12)$$

$$\phi_M \equiv 0 \text{ at } x = 0 \text{ (positive current collector)} \quad (13)$$

where $exm$ is the tortuosity exponent, and $\sigma$ the conductivity of the solid phases (constant for each electrode).

### 3.3. Electrode kinetics

$$\frac{\partial i_L}{\partial x} = j_{HR} + j_{NR} \text{ in POS, NEG} \quad (14)$$

where $j_{HR}$, $j_{NR}$ are the transfer current densities (in A/cm$^3$) of charge/discharge and water-electrolysis reactions, respectively:

$$j_{HR} = j_{0,HR}a_{max}\left(\frac{c}{c_{ref}}\right)^{\gamma}\left(\frac{\epsilon-\epsilon_{min}}{\epsilon_{max}-\epsilon_{min}}\right)^{\zeta_1}\left(\frac{\epsilon_{max}-\epsilon}{\epsilon_{max}-\epsilon_{min}}\right)^{\zeta_2\theta(I)} \times\left[\exp\left(\alpha_{HR}\frac{n_{HR}F}{RT}\eta_{D,HR}\right) - \exp\left(-(1-\alpha_{HR})\frac{n_{HR}F}{RT}\eta_{D,HR}\right)\right] \quad (15)$$

$$j_{NR} = j_{0,NR}a_{max}\left(\frac{\epsilon-\epsilon_{min}}{\epsilon_{max}-\epsilon_{min}}\right)^{\zeta_1} \times\left[\exp\left(\alpha_{NR}\frac{n_{NR}F}{RT}\eta_{D,NR}\right) - \exp\left(-(1-\alpha_{NR})\frac{n_{NR}F}{RT}\eta_{D,NR}\right)\right] \quad (16)$$

$$\theta(I) = \begin{cases} 0 \text{ if } I \le 0 \text{ (discharge)} \\ 1 \text{ if } I > 0 \text{ (charge)} \end{cases}$$

$$\eta_{D,HR} = \phi_M - \phi_L - \phi_{0,HR};\ \eta_{D,NR} = \phi_M - \phi_L - \phi_{0,NR}$$

$$i_L = I \text{ in RES, SEP, at inner borders} \quad (17)$$

$$i_L = 0 \text{ at current collectors} \quad (18)$$

where $j_0$ is the exchange current density for flat electrodes (fully-charged, at concentration $c_{ref}$), $a_{max}$ the specific surface per volume unit of fully-charged porous electrodes, $\gamma$ the reaction order, $\zeta_1$ and $\zeta_2$ the passivation exponents (cf. [12]), $\alpha$ the charge-transfer coefficient, $n$ the charge number, $m$ the molality, and the quotient $(\epsilon-\epsilon_{min})/(\epsilon_{max}-\epsilon_{min})$ corresponds to the SOC.

### 3.4. Ion transport

$$\epsilon\frac{\partial c}{\partial t} = -c\frac{\partial\epsilon}{\partial t} + \frac{\partial}{\partial x}\left(\epsilon^{ex}D\frac{\partial c}{\partial x}\right) + \frac{3-2t_+^0}{2F}j_{HR} + \frac{1-t_+^0}{F}j_{NR} \text{ in POS} \quad (19)$$

$$\epsilon\frac{\partial c}{\partial t} = -c\frac{\partial\epsilon}{\partial t} + \frac{\partial}{\partial x}\left(\epsilon^{ex}D\frac{\partial c}{\partial x}\right) + \frac{1-2t_+^0}{2F}j_{HR} + \frac{1-t_+^0}{F}j_{NR} \text{ in NEG} \quad (20)$$

$$\epsilon\frac{\partial c}{\partial t} = \epsilon^{ex}D\frac{\partial^2 c}{\partial x^2} \text{ in RES, SEP} \quad (21)$$

$$\epsilon^{ex}\frac{\partial c}{\partial x} \text{ continuous, at inner borders} \quad (22)$$

$$\frac{\partial c}{\partial x} = 0 \text{ at current collectors} \quad (23)$$

where $D$ is the diffusion constant.

### 3.5. Structural change of electrodes (porosity)

$$\frac{\partial\epsilon}{\partial t} = \frac{\Delta V_m}{nF}\cdot j_{HR} \text{ in POS, NEG} \quad (24)$$

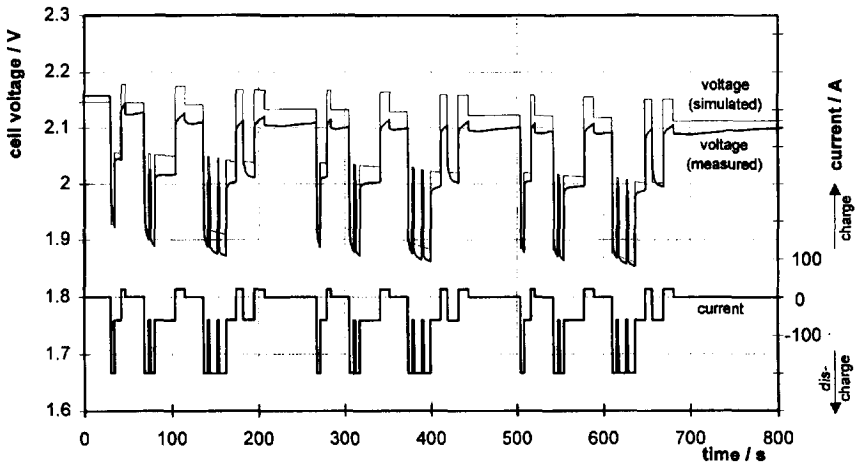


Fig. 2. ECE-cycle current pattern: simulation and experimental data.

$$\Delta V_m = V_m(PbSO_4) - V_m(PbO_2) \text{ in POS}$$

$$\Delta V_m = V_m(PbSO_4) - V_m(Pb) \text{ in NEG}$$

$$\epsilon = \epsilon_{RES} \text{ in RES} \quad (25)$$

$$\epsilon = \epsilon_{SEP} \text{ in SEP} \quad (26)$$

where $V_m$ is the molar volume of active materials (charged/discharged).

### 3.6. Empirical parameters

These equations contain about 25 empirical parameters such as conductivities, exchange-current densities, charge-transfer coefficients, or specific electrode surfaces. These values vary over a wide range in different published simulations [6,12,17,18]. Recent work [16] shows that systematic determination of these parameters is difficult even using destructive measurements of porosity distributions, etc., which are almost impossible to execute by a battery user. In this work, those parameters were taken from the open literature.

## 4. First simulation results

The PDE set mentioned above was simulated on a Pentium PC using the Newton–Raphson method with implicit time-step [19]. First, constant-current discharges with different currents were applied to the battery and simulated. Good coincidence between measured and simulated $U(t)$ can be achieved by proper choice of parameters.

Next, the voltage response of the battery model after switching off the constant current is considered. Simulation results typically differ from measured voltages. The instantaneous voltage drop due to ohmic and transfer resistance is calculated too high, whereas concentration overpotential with its slow decay is underestimated. No set of parameters could be found improving this situation substantially.

Finally, current patterns were defined in order to simulate operating conditions of electric vehicles including regenerative braking. They are based on the ECE cycle, a standard test procedure primarily defined for vehicles with internal combustion engine. Fig. 2 shows the example. The simulation slightly overestimates the voltage drop immediately after a current step, but after that the simulated voltage is too flat compared with experimetal data. This discrepancy may be attributed to an underestimation of the concentration overpotential, again. Further work will result in more realistic calculation of overvoltages after systematic determination of the parameters.

## 5. Conclusions

Single-pore and macrohomogeneous approaches for one-dimensional modelling of batteries are essentially equivalent. Simulating a VRLA traction battery using a one-dimensional macrohomogeneous model showed that this model type is well suited for modelling batteries not only under constant-current coditions, but also under operating conditions of electric vehicles. An important uncertainty of mesoscopic models lies in the determination of empirical parameters which would require systematic measurements and which limits the achievable accuracy of model predictions.

Several refinements of the model equations are desirable. Double-layer capacity should be represented because it forms an RC element with a time constant in the order of $10^{-1}$ s. Oxygen cycle (electrolysis and recombination) should be implemented. The concentration overpotential is underestimated in the present model. Electrolyte exchange with the volume outside the stack of plates may be included by expansion of the one-dimensional model.

For many practical purposes, e.g. on-board battery management, or simulation of the electric 12 V supply of vehicles, time consumption for numerically solving PDE systems will be unacceptable, and simplifications will have to be made which reduce this model to a set of ordinary differential equations (ODE).

Ekdunge [20] suggests a quasi-macrohomogeneous model with just three volume elements (positive electrode, separator, negative electrode) and simplified effective transport and reaction properties.

Another approach which might be regarded as a simplified mesoscopic model is an impedance model in the frequency domain which describes diffusion compartments as generalized Warburg elements [21]. In practice, it is necessary to deal with finite current steps in the time domain, though this equivalent circuit model consists of nonlinear and frequency-dependent elements, cf. Ref. [22].

In addition, such simplifications will reduce the number of empirical parameters. However, the resulting model will be closer to the electrochemical laws governing the behaviour of the battery, and thus more general than a purely phenomenological approach.

## References


[1] R. de Levie, *Adv. Electrochem. Electrochem. Eng.*, *6* (1967) 329–397.
[2] J. Newman and W. Tiedemann, *AIChE J.*, *21* (1975) 25–41.
[3] R.R. Nilson, *J. Power Sources*, *41* (1993) 25–53.
[4] E. Meissner, *J. Power Sources*, *42* (1993) 103–118.
[5] A. Winsel, *Ber. Bunsenges.*, *79* (1975) 827–836.
[6] T.V. Nguyen and R.E. White, *Electrochim. Acta*, *38* (1993) 935–944.
[7] O. Lanzi and U. Landau, *J. Electrochem. Soc.*, *137* (1990) 585–593.
[8] W.G. Sunu, Mathematical model for design of battery electrodes, lead–acid cell modeling, in R.E. White (ed.), *Electrochemical Cell Design*, Plenum, New York, 1984, pp. 357–376.
[9] R.M. LaFollette and D.N. Bennion, *J. Electrochem. Soc.*, *137* (1990) 1670–1681.
[10] P. Ekdunge and D. Simonsson, *J. Appl. Electrochem.*, *19* (1989) 136–141.
[11] P. Ekdunge and D. Simonsson, *J. Appl. Electrochem.*, *19* (1989) 127–135.
[12] H. Gu, T.V. Nguyen and R.E. White, *J. Electrochem. Soc.*, *134* (1987) 2953–2960.
[13] D.M. Bernardi, *J. Electrochem. Soc.*, *137* (1990) 3701–3707.
[14] D. Simonsson, *J. Appl. Electrochem.*, *3* (1973) 261–271.
[15] R.R. Nilson and R.I. Chaplin, *J. Power Sources*, *41* (1993) 13–23.
[16] J. Landfors, D. Simonsson and A. Sokirko, *J. Power Sources*, *55* (1995) 217–230.
[17] T.V. Nguyen, R.E. White and H. Gu, *J. Electrochem. Soc.*, *137* (1990) 2998–3004.
[18] Z. Mao, R.E. White and B. Jay, J. Electrochem. Soc., *138* (1991) 1615–1620.
[19] W.H. Press, S.A. Teukolsky, W.T. Vetterling and Brian P. Flannery, *Numerical Recipes in C, The Art of Scientific Computing*, Cambridge University Press, Cambridge, 2nd edn., 1992.
[20] P. Ekdunge, J. Power Sources, *46* (1993) 251–262.
[21] P. Mauracher, E. Karden and K. Rembe, Measurement of the ultra-low frequency impedance of lead–acid batteries, *LABAT'96, Varna, Bulgaria, 3–6 June 1996.*
[22] P. Mauracher and E. Karden, Dynamic modeling of lead–acid batteries using impedance spectroscopy for parameter identification, *5th European Lead Battery Conf. (5ELBC), Barcelona, Spain, 1–4 Oct. 1996.*